May 2002

Magnetic force microscopy observations of the magnetic behavior in Co–C nanodot arrays

L. Gao
University of Nebraska - Lincoln

Sy_Hwang Liou
University of Nebraska-Lincoln, sliou@unl.edu

M. Zheng
University of Nebraska - Lincoln

Ralph Skomski
University of Nebraska-Lincoln, rskomski2@unl.edu

M.L. Yan
University of Nebraska - Lincoln

See next page for additional authors

Magnetic force microscopy observations of the magnetic behavior in Co–C nanodot arrays

L. Gao, S. H. Liou,[a] M. Zheng,[b] R. Skomski, M. L. Yan, and D. J. Sellmyer
Department of Physics and Astronomy and Center for Materials Research and Analysis, University of Nebraska, Lincoln, Nebraska 68588

N. I. Polushkin
Institute for Physics of Microstructures, Russian Academy of Sciences, 603600 GSP-105 Nizhni Novgorod, Russia

The nanomagnetic behavior of Co–C nanodot arrays was investigated by magnetic force microscopy (MFM) and an alternative gradient force magnetometer. The direction of the easy axis can be observed directly with MFM by comparing the saturated magnetization state and the remanent magnetization state. Interaction of the domain wall with local defects was observed by field dependent MFM measurements. Some types of defects that can pin domain wall movement were identified. © *2002 American Institute of Physics.* [DOI: 10.1063/1.1452259]

I. INTRODUCTION

The investigation of magnetic nanodot arrays is one of the exciting fields in materials science. Many methods being used to produce nanodot arrays are ion-beam[1] or indirect lithography.[2–4] Recently, we showed that magnetic nanodot arrays could be generated by directly exposing Co–C films to an interferometric laser.[5,6] Co–C films were chosen because the metastable Co carbides decompose easily into Co and C upon annealing and form a simple system with immiscible magnetic and nonmagnetic phases.[7–10] As-deposited Co–C films may contain tiny superparamagnetic Co or Co-rich clusters.[5,6] The Co atoms rearrange upon laser annealing and form more strongly interacting magnetic Co or Co-rich clusters in regions where the laser intensity is highest.[5,6] The magnetic nanodots can be embedded either in a paramagnetic or magnetic matrix (regions between the dots) depending on the power of laser being used.[6] In this work, we focus on a sample in which the dots exhibit ferromagnetic order and are embedded in a magnetic matrix in which the magnetization is lower than that of the nanodots. Magnetic force microscopy (MFM) was used to study the magnetic anisotropy and domain-wall motion behavior of Co–C nanodot arrays.

II. EXPERIMENTS

Details of the sample preparation were reported in previous work.[5,6] The $Co_{50}C_{50}$ (at. %) films were cosputtered onto a water-cooled 7059 glass substrate and had a thickness of 20 nm. Periodic magnetic nanodot arrays were produced by direct lithography using an interferometric laser.

Magnetic hysteresis loops were measured by an alternative gradient force magnetometer (AGFM). The domain pattern was observed by a MFM. An electromagnet was used to apply a variable magnetic field on the sample. All the magnetic images were obtained using a MFM with low magnetic stray field and high-coercivity MFM tips.[11] The tips were fabricated by deposition of 7 nm of CoPt films. The low stray field made the influence of magnetic tips on the sample negligible. The tip's magnetization points downward about 10° off the tip direction, that is, perpendicular to the sample surface. These MFM images, taken with a vertically magnetized tip, highlight the out-of-plane component of the dots' magnetization. The light and dark contrast corresponds to the strength of the stray field gradient on the sample's surface. The light color represents a positive phase shift of the MFM tip (i.e., the interaction between the sample and the MFM tip is repulsive).

III. RESULTS AND DISCUSSION

Figure 1(a) shows a plane view of Co–C nanodot arrays. The dots have a diameter of about 250 nm and a center-to-center spacing of about 500 and 900 nm as marked. In Fig. 1(a), the external field was applied horizontally. Figures 1(b) and 1(c) are MFM images of the saturated and remanent states, respectively, of the nanodot arrays. Figure 1(b) was taken under a field of 425 Oe after the sample was completely saturated under a field of 1200 Oe. The images remain the same at 1200 and 425 Oe. According to the magnetization direction of the tip and the MFM contrast mechanism, the magnetization-direction of the nanodot arrays is from dark to light. In the saturated state, all the dots were magnetized along the field direction, as shown in Fig. 1(b). The field was then removed and the MFM image of the remanent state was obtained [Fig. 1(c)]. The magnetization direction of nanodot arrays did not change and was still along the direction of the applied magnetic field. Since the magnetization direction should change to the nearest easy axis after the applied magnetic field is removed, the present applied field direction is the easy axis direction [marked in Fig. 1(a)]. In order to verify the easy axis direction, we applied the field along a direction 30° off the easy axis by rotating the sample clockwise from the direction where Fig.

[a]Author to whom correspondence should be addressed; electronic mail: sliou@unl.edu
[b]Present address: MMC Technology, San Jose, CA 95131; electronic mail: minzheng@mmctechnology.com

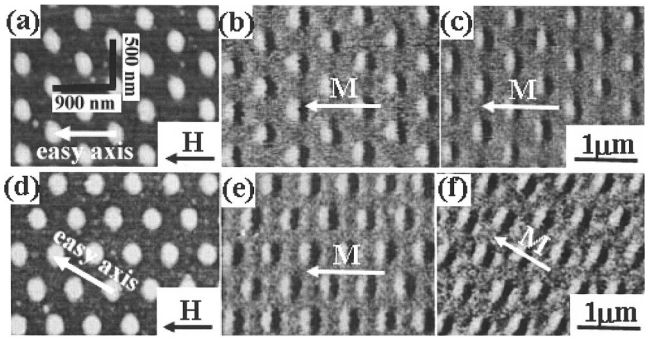

FIG. 1. AFM and MFM images of Co–C nanodot arrays. The top three images were measured with field applied along the easy axis direction. (a) AFM image, (b) MFM image in the saturated state under a 425 Oe field, (c) MFM image in the remanent state. The bottom three images were measured with field applied along the direction 30° off easy axis. (d) AFM image, (e) MFM image in the saturated state under a 425 Oe field, (f) MFM image in the remanent state.

1(a) was taken. Figure 1(d) shows an atomic force microscopy (AFM) image of Co–C nanodot arrays. The angle between the applied field direction and the easy axis is about 30°. Figures 1(e) and 1(f) were taken the same way as Figs. 1(b) and 1(c), respectively. In saturated states, there is no difference between Figs. 1(b) and 1(e). However, after the field was removed, shown in Fig. 1(f), the direction of magnetization of the nanodot arrays changed by about 30° and returned to the easy axis direction. The above result shows that we can use MFM to observe local magnetic behavior microscopically.

Figure 2 shows ferromagnetic hysteresis loops of Co–C nanodot arrays with the applied magnetic field parallel to the plane of the sample. Hysteresis loop (a) was measured with the applied field along the easy axis direction, corresponding to the AFM image in Fig. 1(a). The coercivity of this direction is 100 Oe and the remanent ratio (M_r/M_s) is 0.86. Hysteresis loop (b) was measured with the applied field along the direction 30° off the easy axis, corresponding to the AFM image in Fig. 1(d). The coercivity of this direction is 87 Oe and the remanent ratio is 0.72. The ratio of the remanent magnetization $[M_r(\mathrm{b})/M_r(\mathrm{a})]$ calculated from two hysteresis loops is 0.840. This value is very close to the 0.866 (or cos 30°) that is expected from a change in magnetization direction and is consistent with the easy axis of Co–C nanodot arrays observed by MFM.

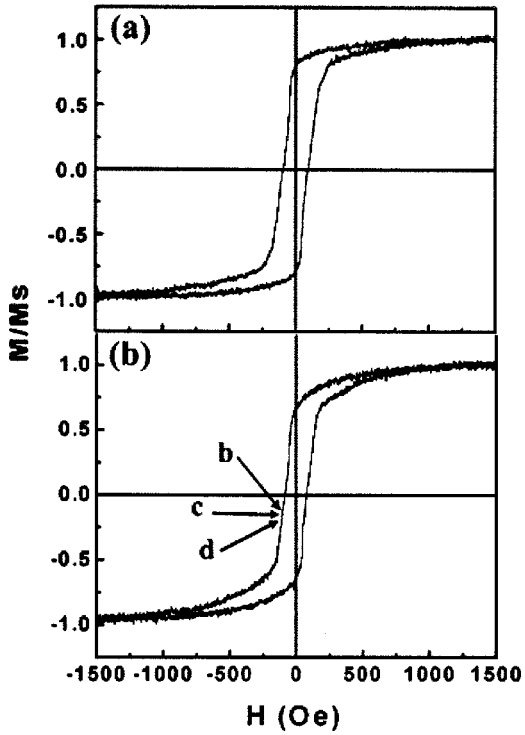

FIG. 2. Hysteresis loops of Co–C nanodot arrays with the field applied (a) along the easy axis direction and (b) along the direction 30° off easy axis. Points (b), (c), and (d) in (b) correspond to the fields in Figs. 3(b)–3(d), respectively.

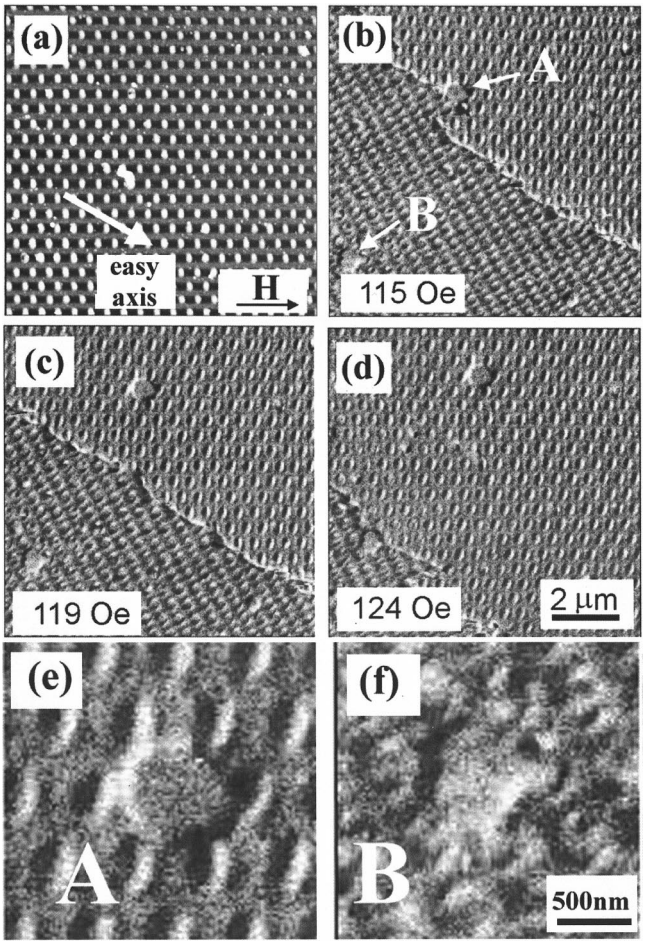

FIG. 3. Domain-wall motion behavior of Co–C nanodot arrays. (a) AFM image, (b) MFM image under a 115 Oe field, (c) MFM image under a 119 Oe field, (d) MFM image under a 124 Oe field. A and B are magnetic defects. (e), (f) magnified defects A and B under a 119 Oe field. The magnetization of A points to the left and the magnetization of B points to the right.

When the applied magnetic field is near the coercive field, domain-wall motion behavior can be observed, as shown in Fig. 3. The applied field is from 115 to 124 Oe, corresponding to points (b), (c) and (d) in Fig. 2(b). Figure 3(a) shows an AFM image of the uniform nanodot arrays. The applied field and easy axis directions are shown. The applied magnetic field causes domain-wall motion, as shown in Figs. 3(b)–3(d). In Fig. 3(b), the magnetic responses of

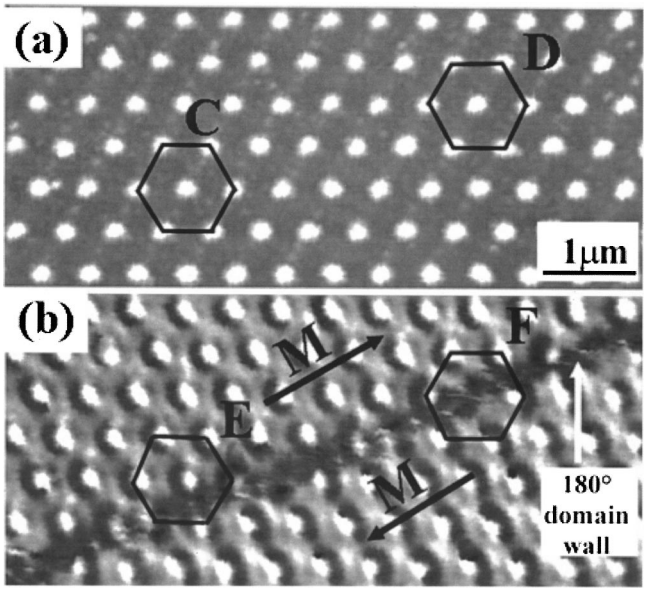

FIG. 4. (a) Topographic image and (b) MFM image of a 180° domain wall in Co–C nanodot arrays. The domain wall is located in the matrix, shown in hexagon E, and on the dot, shown in F. Hexagons C and D are corresponding hexagons in the AFM image.

two areas marked ''A'' and ''B'' are different while there is no special features in the AFM image [Fig. 3(a)]. The defects at areas A and B are likely magnetic in origin. Magnified defects A and B under the 119 Oe field are shown in Figs. 3(e) and 3(f). From the light and dark contrast, the magnetization direction of area A is opposite to the applied magnetic field direction and the magnetization direction of area B is along the applied magnetic field direction. This can be explained if area A has a higher coercive field than its neighbor and area B has a lower coercive field than its neighbor. As shown in Figs. 3(b) and 3(d), we observed that the domain-wall was pinned around areas A and area B. This indicates that both soft and hard magnetic regions are essentially pinning sites. Some domain walls with a zigzag shape appear in Fig. 3(c). This may also be explained if there is a distribution of the switching magnetic field in the nanodots. All these indicate that the magnetic inhomogeneity in the sample contributed to the domain wall pinning.

Figure 4 shows AFM and MFM images of a region with an 180° domain wall. Figure 4(a) shows a topographic image of Co–C nanodot arrays. There is no significant difference between hexagons ''C'' and ''D.'' Figure 4(b) is the MFM image of the remanent state (after an ac demagnetization field). The reversed contrast of the dots shows the existence of the 180° domain wall (indicated by a white arrow). Nanodots and the matrix form ''macrodomains'' (indicated by black arrows). By comparing hexagons ''E'' and ''F'' in Fig. 4(b), we observe that the domain wall is located not only on the matrix (shown in hexagon ''E'') but also on the dot (shown in hexagon F). This reveals that the matrix is ferromagnetic and that the dots on the domain wall are not single domain.

IV. CONCLUSION

In summary, these experiments show that we can use MFM to observe local magnetic behavior microscopically. We can illustrate the easy axis direction by comparing the saturated state and remanent state magnetization directions at different applied field directions. Domain-wall pinning by the local defects was observed by field dependent MFM measurements. The defect is likely magnetic in origin. The domain walls are located on both the dots and the matrix, which indicates that the matrix is ferromagnetic and that the domain structures of dots on the domain wall are not single domain.

ACKNOWLEDGMENTS

This research was supported by the Army Research Office (ARO) Grant No. DAAD19-00-1-0119, and by the Department of Energy (DOE), Nebraska Research Institute (NRI), and Center for Materials Research and Analysis (CMRA).

[1] B. D. Terris, L. Folks, D. Weller, J. E. E. Baglin, A. J. Kellock, H. Rothuizen, and P. Vettiger, Appl. Phys. Lett. **75**, 403 (1999).
[2] S. Y. Chou, M. Wei, P. R. Krauss, and P. B. Fisher, J. Vac. Sci. Technol. B **12**, 3695 (1994).
[3] T. A. Savas, M. Farhoud, H. I. Smith, M. Hwang, and C. A. Ross, J. Appl. Phys. **85**, 6160 (1999).
[4] A. Fernandez, P. J. Bedrossian, S. L. Baker, S. P. Vernon, and D. R. Kania, IEEE Trans. Magn. **32**, 4472 (1996).
[5] M. Zheng *et al.*, Appl. Phys. Lett. **79**, 2606 (2001).
[6] M. Zheng *et al.*, IEEE Trans. Magn. **7**, 2070 (2001).
[7] M. Yu, Y. Liu, and D. J. Sellmyer, J. Appl. Phys. **85**, 4319 (1999).
[8] T. J. Konno and R. Sinclair, Acta Metall. Mater. **42**, 1231 (1994).
[9] T. Hayashi, S. Hirono, M. Tomita, and S. Umemura, Nature (London) **381**, 772 (1996).
[10] J.-J. Delaunay, T. Hayashi, M. Tomita, and S. Hirono, J. Appl. Phys. **82**, 2200 (1997).
[11] S. H. Liou and Y. D. Yao, J. Magn. Magn. Mater. **190**, 130 (1998).